RSC Advances

ROYAL SOCIETY OF CHEMISTRY

www.rsc.org/advances

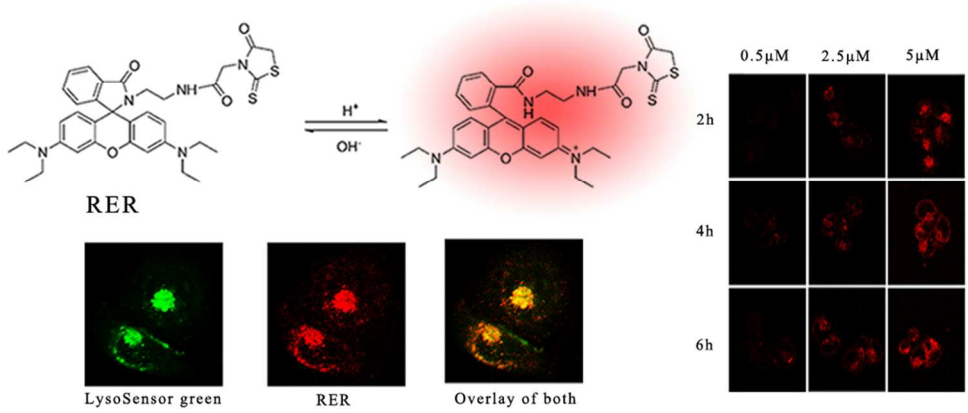

A novel pH probe based on rhodamine-rhodanine platform

A novel pH probe based on rhodamine-rhodanine platform
90x44mm (300 x 300 DPI)

Journal Name

RSCPublishing

ARTICLE

Cite this: DOI: 10.1039/x0xx00000x
Received 00th January 2012,
Accepted 00th January 2012
DOI: 10.1039/x0xx00000x
www.rsc.org/

A novel pH probe based on rhodamine-rhodanine platform

Xuan-Xuan Zhao[a, †], Xin-Peng Chen[b, †], Shi-Li Shen[a], Dong-Peng Li[a], Shuai Zhou[a], Ze-Quan Zhou[a], Yu-Hao Xiao[a], Gang Xi[a], Jun-Ying Miao[b,*], Bao-Xiang Zhao[a,*]

We developed a rhodamine-rhodanine-based pH probe with pKa = 4.85 in buffer solution. The fluorescent intensity exhibited strong pH-dependent performance and responded linearly to minor pH fluctuations within the range of 4.2-5.2. In addition, the fluorescent microscopic images suggested this probe had excellent cell membrane permeability and could image weak acid pH changes of lysosome in live cells without auto-fluorescence and interference from the complex intracellular environment. The results demonstrated that the probe had great potential in monitoring H^+ in vitro and in living cells.

Introduction

Hydrion, one of the most common cations, plays a critical role in cell growth [1, 2], proliferation [3], apoptosis [4], autophagy [5, 6], ion transport [7], inflammation and tumor growth [8], and other cellular processes. As an important indication of cellular health, minor variations of intracellular pH may cause cellular dysfunction and serious diseases, such as colorectal cancer [9], breast cancer [10], cystic fibrosis [11], neurodegenerative disorders [12] even Alzheimer's disease [13-15].

In view of the psychological significance of pH in biological system, accurately detecting the distribution and concentration of H^+ with high spatiotemporal resolution in various cellular and physiological compartments has become increasingly important. Recently, fluorescent probes have become the promising tools for quantitatively measuring intracellular pH because of their good selectivity, high sensitivity, operational simplicity, low cost and real time monitoring [16-18]. Moreover, the fluorescence microscopy can provide us with the spatial-temporal distribution of H^+ within living cells [19-21].

The previous reported pH fluorescence probes can be mainly divided into two classes: one type for cytosol that works in the pH range from 6.8 to 7.4, and the other type for acidic organelles such as lysosomes and endosomes [13, 22] which functions at pH 4.5-6.0. However, the frequent pH fluorescence probes suffer from several drawbacks, such as the pKa value is highly dependent on ionic strength of solution [23], fluorescent lifetime and quantum yield relied heavily on solvent polarity [24], even some pH probes need to be excited by high-energy radiation [25], and some other questions like photostability or interference of auto-fluorescence and photobleaching [26-28]. In addition, there are few pH probes used for acidic organelles, though they play critical role in vital movement [29-34] Therefore, developing desirable acidic pH probes, which can respond observably to a minor pH change, give reliable results, and effectively avoid interference from native cellular species particularly, has attracted extensive attention. Among the familiar fluorophores that could be potentially used to design pH probes, rhodamine framework has particular photophysical advantages in biological application because of its high fluorescence quantum yield, relatively long absorption and emission wavelengths elongated to the visible region, large absorption coefficient and great photostability. Rhodamine-based fluorescent probes can remarkably distinguish target ion or molecular from other species based on the change in structure between spirocyclic and open-cycle forms [34-38]. As to the rhodamine-based pH fluorescence probes, these spirocyclic compounds are non-fluorescent and colorless under neutral and basic conditions, while upon binding to specific analytes, namely H^+, the spirocyclic form will open to restore the fluorescence intensity along with pink color because the spirocyclic structure is highly sensitive to the pH of the solutions. Though many rhodamine-based pH probes have been exploited, some of them need a large amount of organic solvents to increase its solubility [23, 39]. Therefore, to develop new rhodamine-based pH probes with excellent water solubility has come into question.

Generally, an amine-containing side was used to design a lysosome-specific pH probe, which can help the probe to accumulate in the acidic environment selectively [29, 40-42]. However, even though the protonation of the amino can induce a remarkable fluorescence change through the redistribution of the charge, it was difficult to avoid "alkalizing effect" of the amino side chain which would increase lysosomal pH after long incubation with the probe [43]. To overcome this disadvantage, decreasing the amount of aliphatic amine seems to be valid as well [36, 44]. Therefore, a novel pH probe **RER** was designed by introducing a rhodanine moiety through an amide functional group to prevent the "alkalizing effect". To the best of our knowledge, the introduction of rhodanine to a fluorescent probe for sensing pH in living cells is still barely explored [45].

With these criteria in mind, we designed and synthesized a new pH probe **RER** to detect H^+ in biological systems through a fast ring-opening of spiro structure in rhodamine fluorophore. The probe displays remarkable fluorescence intensity enhancement and obvious

color variation from colorless to pink with the pH from 7.2 to 4.0. Moreover, the pKa value 4.85 implied that **RER** was appropriate for studying acidic organelles such as lysosomes without native cellular species interference in biological systems. The introduction of the rhodanine structure to the probe improved the cell membrane permeability, photo-stability and even helped to decrease the cytotoxicity of the probe to the HeLa cells, which shows that **RER** is indeed a ponderable.

Results and discussion

Design and synthesis of RER

As shown in Scheme 1, probe **RER** was designed based on the excellent photophysical properties of rhodamine and the transformation in structure between spirocyclic (non-fluorescent) and ring-opening (fluorescent) forms responding to H^+. **RER** was synthesized by treating rhodamine B with ethylenediamine followed by rhodanine-3-acyl chloride. After column chromatography on silica gel using DCM : MeOH (30:1, v/v) and recrystallized from EtOH, **RER** was obtained in 41% yield and confirmed by IR, ^{1}H NMR, ^{13}C NMR and HRMS spectra (Electronic Supplementary Information, † ESI). In view of the colorless and non-fluorescence of **RER** in neutral solution, the probe is envisioned to turn on when the H^+ is introduced as a signal switcher. The solution of **RER** in B-R buffer/EtOH (8/2, v/v, pH = 7.2) was colorless and non-fluorescent, which confirmed that **RER** exists in a spirolactam form. This consideration is also supported by the characteristic peak of the spirocycle carbon (chemical shift at 64.5 ppm) in the ^{13}C NMR spectra (Fig. S7).

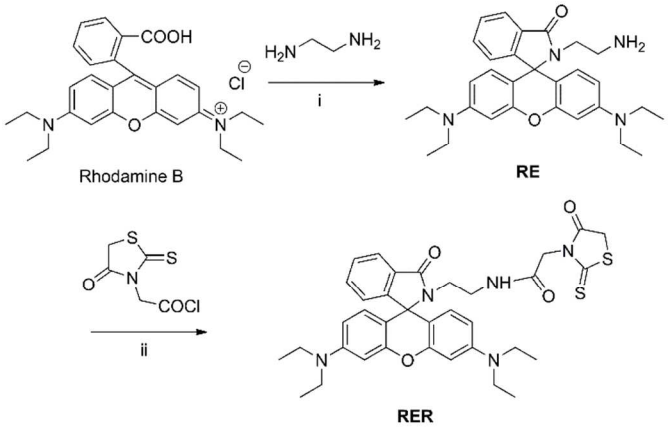

Scheme 1 (i) EtOH, reflux, 9 h, 87% (ii) CH_2Cl_2, rt, 2 h, 41 %

Spectroscopic properties and optical responses to pH

All samples were performed in a mixture solution (B-R buffer-EtOH, v/v = 8:2 for fluorescence and 7:3 for UV-vis) and waited for 2 h before measurement.

There is almost no absorption in the range of 540-580 nm near neutral pH, however, with decreasing the pH from 5.0 to 3.4, UV-vis absorption of the rhodamine moiety gradually increased at 560 nm (Fig. S1). Meanwhile, the solution changed from colorless to pink, indicating that **RER** could serve as a "naked-eye" indicator for acidic pH.

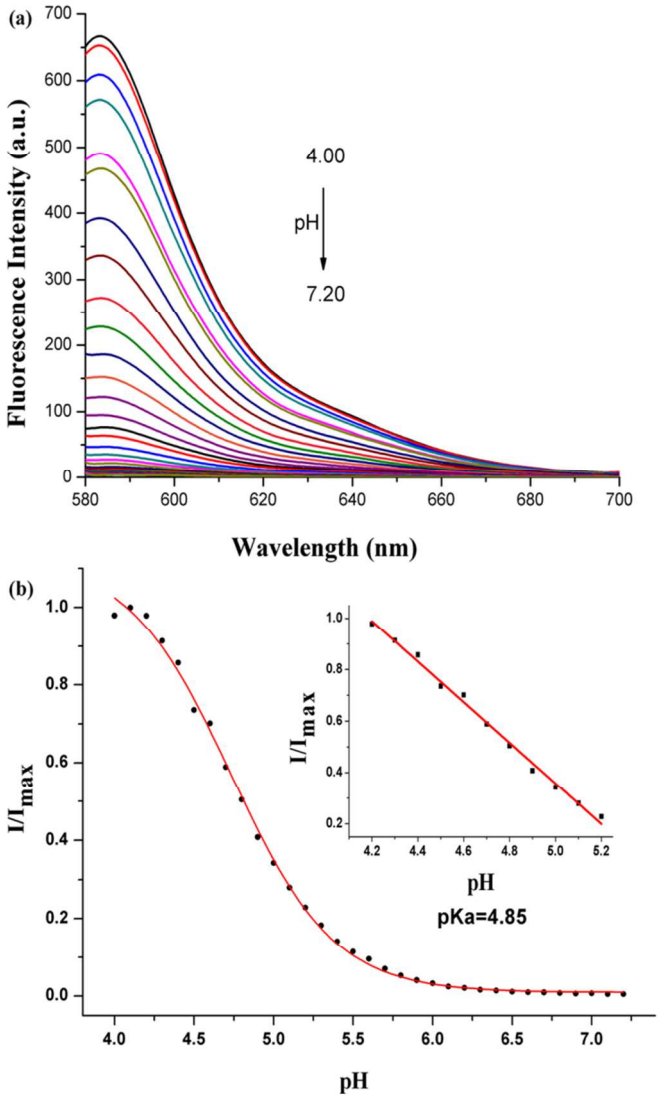

Fig. 1 (a) Change of the fluorescence spectra of **RER** (1 μM) in aqueous solution containing ethanol (B-R buffer-EtOH, v/v = 8:2) with decreasing pH from 7.2 to 4.0 (λex = 561 nm). (b) Sigmoidal fitting of the pH-dependent fluorescence intensity at 583.5 nm. Inset: the good linearity in the pH range of 4.2-5.2.

The fluorescence property of **RER** as a function of pH is displayed in Fig. 1. **RER** exhibits almost no emission peak centred at 583.5 nm under neutral conditions with an excitation wavelength of 561 nm. However, by decreasing the pH of **RER** solution, a remarkably fluorescence turn-on response is observed. The fluorescence intensity of probe **RER** (1 μM) enhanced when the pH decreased from 7.2 to 4.0 (Fig. 1). A good linearity (R^2 = 0.99381) between fluorescent intensity and pH ranging from 4.2 to 5.2 was obtained according to fluorescence titration. The analysis of fluorescence intensity changes as a function of pH using the Henderson-Hasselbalch equation calculated a pKa of 4.85, suggesting that **RER** may serve as a functional pH probe for weak acidic organelles in vivo like lysosome. The fluorescence quantum yield of **RER** at pH 4.5 was determined to be 0.69 (rhodamine B as a standard) [46].

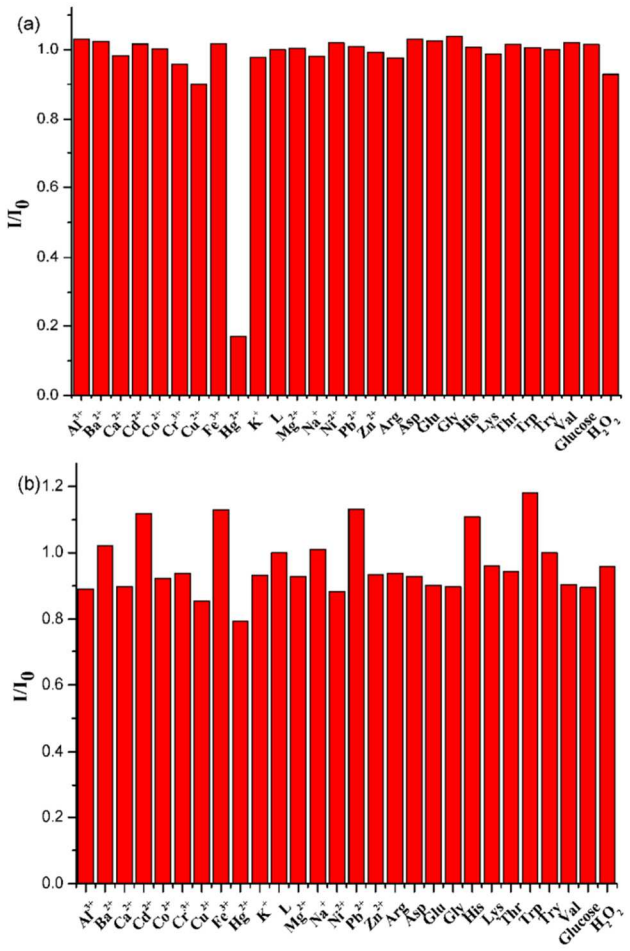

Fig. 2 Relative fluorescence intensity at 583.5 nm of **RER** (1 μM, λex = 561 nm) in the presence of diverse metal ions in aqueous solvents containing ethanol (B-R buffer-EtOH, v/v = 8:2) at pH 4.5 (a) and pH 7.0 (b), K^+ (1 mM), Na^+ (1 mM), Ca^{2+} (0.1 mM), Mg^{2+} (0.1 mM), Cu^{2+} (50 μM), Hg^{2+} (50 μM), Fe^{3+} (50 μM), Al^{3+} (50 μM), Zn^{2+} (50 μM), Co^{2+} (50 μM), Ni^{2+} (50 μM), Cr^{3+} (50 μM), Cd^{2+} (50 μM), Pb^{2+} (50 μM), Ba^{2+} (50 μM), histidine (0.2 mM), tyrosine (0.2 mM), aspartic acid (0.2 mM), arginine (0.2 mM), glutamic acid (0.2 mM), lysine (0.2 mM), tryptophan (0.2mM), threonine (0.2 mM), valine (0.2mM), glycine (0.2 mM), glucose (1 mM), H_2O_2 (2 mM).

To test the practical application of **RER**, the interference experiment was performed to estimate the influence caused by various metal ions (Na^+, K^+, Ca^{2+}, Hg^{2+}, Al^{3+}, Ba^{2+}, Zn^{2+}, Co^{2+}, Pb^{2+}, Mg^{2+}, Ni^{2+}, Cu^{2+}, Cr^{3+}, Cd^{2+}, Fe^{3+}), which may be present in the systems being analyzed. Moreover, some other bioactive small molecules (His, Tyr, Trp, Asp, Val, Arg, Glu, Lys, Thr, Gly, Glucose and H_2O_2) were also tested (Fig. 2). At pH = 4.5 (Fig. 2 (a)), there was no observed effect on fluorescence intensity within the additives except for Hg^{2+} caused fluorescence quenching to some degree. However, this quenching should not affect the application of the probe since the contents of Hg^{2+} is very little within cells. At pH = 7.0 (Fig. 2 (b)), the addition of those analysts caused no appreciable spectroscopic changes under the testing conditions. Therefore, probe **RER** could be used to respond to weakly acidic pH without interference from the complex intracellular environment.

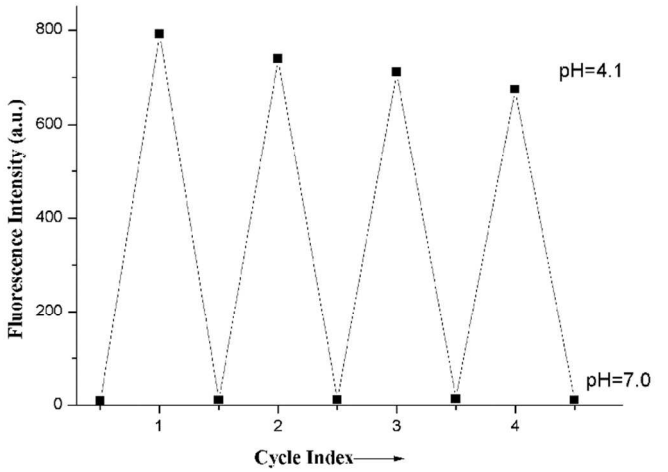

Fig. 3 Reversibility of the fluorescence response at 583.5 nm of **RER** between pH 7.0 and 4.1 (λex = 561 nm).

It is well-known that the reversibility of pH chemosensor is highly required. So the pH value was modulated repeatedly between 4.1 and 7.0 several times, meanwhile the fluorescence intensity of **RER** were recorded. As shown in Fig. 3, the solution was prepared alternately into an acidic solution of pH = 4.1, whereby approximately 85% of the original fluorescence signal was successfully restored after 4 cycles. In contrast, under neutral solution (pH = 7.0), spirocyclic structure of the probe is associated with quenching of the fluorescence. Switching between the fluorescence on/off states can thus be repeated accompanied with the color change repeatedly between pink (pH = 4.1) and colorless (pH = 7.0), which enables us to propose a mechanism for the equilibrium of probe **RER** with variations of pH (Scheme 2). A possible interaction between probe **RER** and H^+ is also suitable for the similar phenomenon in the fluorescence titration plot of other pH probes with the same functional fluorophore as probe **RER** [44, 47-49].

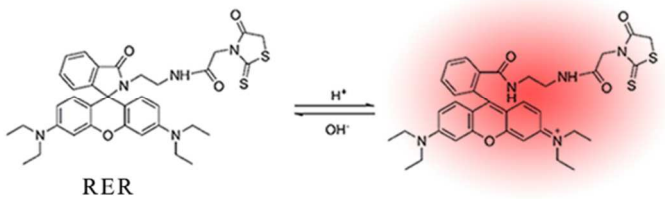

Scheme 2 Proposed mechanism of pH response by protonation and deprotonation of **RER**.

The response time of **RER** to H^+ was tested by measuring the fluorescent response about 2 h (Fig. S2). Images were recorded at intervals of 2 min. The fluorescence of the **RER** solution was weak initially once they were placed in the buffer solution, then the gradual increase of fluorescence intensity was observed at pH 4.1 during the 100 min time-course. The experiment indicates that **RER** can instantly respond to the change of pH since the spirocyclic part of the rhodamine structure is sensitive to the H^+ concentration. It is worth stressing that the fluorescence is stable for a period of time, which supports the deduction that the probe solution reaches a dissociation equilibrium and is not insusceptible to the medium, light, and air. The same experiments at pH 5.3 showed smaller

fluorescence changes, but no significant changes in the fluorescence intensity were observed at pH 7.0. Just as expected, the fluorescence intensities remained stable at pH 4.1, 5.3 and 7.0, respectively, which clarified that **RER** solution could respond to the change of H^+ concentration at various degrees and then keep stable to external environment.

Fluorescence imaging in living cells

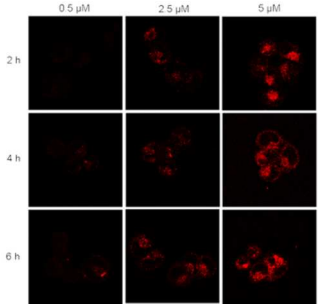

Fig. 4 Fluorescence microscope images of living HeLa cells with different concentrations of **RER** for 2-6 h at 37 °C.

Eventually, living cell imaging assays were performed to investigate whether the probe can sense H^+ sensitively in biological systems. HeLa cells were firstly incubated with different concentrations of **RER** for 2-6 h and then the fluorescence of the probe within the cells was observed by confocal fluorescence microscopy. As shown in Fig. 4, the different fluorescence intensities of **RER** revealed that the probe was membrane-permeable and the response was both time and dose-depended. To further make better understand the distribution of the probe within the cells, the LysosensorTM Green DND-189, an excellent lysosome tracker, was used to stain with the probe. As shown in Fig. 5 (a), after HeLa cells incubated with lysosome tracker (0.5 μM) for 1 h, the visible strong green signals could be collected in the green channel and a long-wavelength emission of cells incubated with **RER** in the red channel was observed (Fig. 5 (b)). The merged image (Fig. 5 (c)) showed convincing yellow fluorescence, which implied the colocalization of **RER** with lysosome. Moreover the long-wavelength emission can greatly reduce the photodamage to the biological components and indicated that the probe **RER** can be used as a long-wavelength emission lysosome sensor. Therefore, a new lysosome-specific probe with better performance was produced.

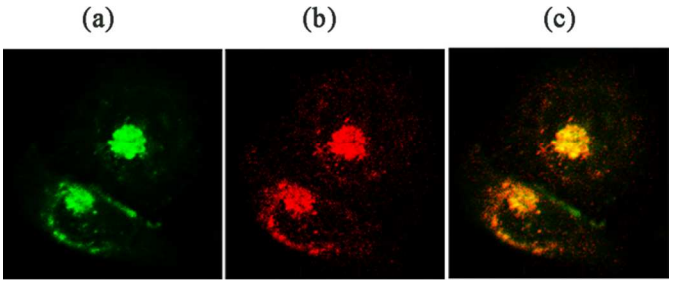

Fig. 5 Fluorescence microscope images of living HeLa cells co-stained with **RER** (10 μM) and LysoSensorTM Green DND-189 (0.5 μM). (a) Green emission from LysoSensor green; (b) Red emission from **RER**; (c) Overlay of (a) and (b), areas of co-localization appeared in yellow.

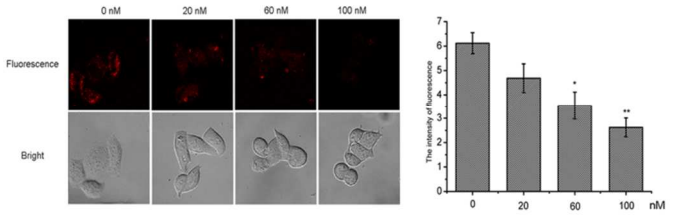

Fig. 6 Fluorescence microscope images of living HeLa cells after incubating with different concentration of bafilomycin A1 (BafA1) and **RER** (5 μM)

Since the pH in lysosome can affect endocytosis, exocytosis, autophagy and other cellular processes [1-7], detection of pH changes in lysosome is of great significance. Considering bafilomycin A1 is a selective inhibitor of the vacuolar-type H^+-ATPase (V-ATPase) to increase lysosomal pH, different concentration of bafilomycin A1 were pre-incubated with HeLa cells for 6 h, then with **RER** (5 μM) for 4 h. The results showed that with increased concentration of bafilomycin A1, the fluorescence intensity gradually weakened. Therefore, **RER** can serve as an efficient fluorescent indicator for lysosomal pH and monitor lysosomal pH changes in living cells.

In addition, to test whether the structure of introduced rhodanine affected the viability of the cells, we explored the cytotoxicity of **RE** and **RER** on HeLa cells by SRB assay protocol (Fig. S3). The cells were incubated with different concentration (1, 5, 10 μM) of **RE** or **RER** respectively for 24 h. Unexpectedly, the high level (10 μM) of **RE** was highly toxic to the cells, while **RER** was almost non-cytotoxicity to HeLa cells at the same experimental conditions, which indicated that the introduced rhodanine part helped to reduce cytotoxicity of the probe.

Finally, considering the fluorescence probe always exerts instability under continuously light irradiation, the photostability of **RER** was investigated in HeLa cells after the cells continuously exposed to irradiation for 5 min. Fluorescence value was quantified by the fluorescence analysis software ImageJ (Fig. S4). The probe presents excellent fluorescence stability in HeLa cells within 5 min.

Experimental

Materials and reagents

All reagents and solvents were purchased from commercial sources and used without further purification. The solutions of metal ions were prepared from nitrate salts which were dissolved in deionized water. Deionized water was used throughout the process of absorption and fluorescence determination. All samples were prepared at room temperature, shaken for 10 s and stood for 2 h before measurement. Britton–Robinson (B-R) buffer was mixed by 40 mM acetic acid, boric acid, and phosphoric acid. Dilute hydrochloric acid or sodium hydroxide was used for tuning pH values. All solvents used in spectroscopic analysis are spectroscopic grade. LysoSensorTM Green DND-189 was used as lysosome tracker (Invitrogen, America).

Apparatus

Thin-layer chromatography (TLC) was conducted on silica gel $60F_{254}$ plates (Merck KGaA). Melting points were determined on an XD-4 digital micro melting point apparatus. ^{1}H NMR spectra were recorded on a Bruker Avance 300 (300 MHz) spectrometer and ^{13}C NMR spectra were recorded on a Bruker Avance 300 (75 MHz) spectrometer, using d_6-DMSO as solvent and tetramethylsilane (TMS) as internal standard. IR spectra were recorded with an IR spectrophotometer VERTEX 70 FT-IR (Bruker Optics). High-resolution mass spectrometry (HRMS) spectra were recorded on a Q-TOF6510 spectrograph (Agilent). Fluorescent measurements were recorded on a Perkin Elmer LS-55 luminescence spectrophotometer and UV–vis spectra were recorded on a U-4100 UV-Vis-NIR Spectrometer (Hitachi). The pH measurements were performed on a PHS-3C digital pH-meter (YouKe, Shanghai, China). The images were obtained using confocal fluorescence microscopy (LSM700) with eye piece 10× magnification and objective 20× magnification. The software ImageJ was used for acquiring the fluorescence values and the data were analyzed by software SPSS 17.0.

Preparation of the probe (RER)

Synthesis of N-(2-(3',6'-bis(diethylamino)-3-oxospiro[isoindoline-1,9'-xanthen]-2-yl)ethyl)-2-(4-oxo-2-thioxothiazolidin-3-yl)acetamide (RER)

Triethylamine (101 mg, 1 mmol) was added to a solution of **RE** (481 mg, 1.0 mmol) in dichloromethane (DCM, 20 mL) under the condition of ice bath. Thereafter a solution of rhodanine acetyl chloride [50, 51] in DCM (5 mL) was added dropwise and the mixture was stirred at room temperature for 2 h. The reaction was quenched with water (20 mL), and extracted with DCM (3 portions of 30 mL). The combined organic layer was washed with water, brine, and dried over anhydrous $MgSO_4$. After the solvent was evaporated, the crude product was purified by column chromatography using DCM/MeOH (30:1, v/v) as an eluent and further recrystallized from EtOH (10 mL) to give the target compound **RER** as light yellow powder in 41 % yield (262 mg). mp: 232-233°C.
IR (KBr), υ: 3446, 3290, 2969, 2926, 1750, 1667, 1614, 1548, 1513, 1397, 1325, 1178, 1119, 817, 786 cm^{-1}; ^{1}H NMR (d_6-DMSO, 300 MHz), δ (ppm): 1.08 (12H, t, J = 6.9 Hz, CH_2CH_3), 2.80 (2H, t, J = 5.1 Hz, CH_2CH_2NH), 3.04 (2H, q, J = 5.1 Hz, CH_2CH_2), 3.32 (8H, q, J = 6.9 Hz, CH_2CH_3), 4.32 (4H, t, J = 6.5 Hz, CH_2 of the rhodanine moiety), 6.37 (6H, d, J = 2.4 Hz, ArH), 6.96-7.01 (1H, ,m, J = 2.7 Hz, ArH), 7.46 (2H, m, J = 3.35 Hz, ArH), 7.77-7.80 (1H, m, ArH), 8.02 (1H, t, J = 5.4 Hz, NH); ^{13}C NMR (d_6-DMSO, 75 MHz), δ (ppm): 12.88, 36.59, 37.69, 39.14, 39.42, 39.70, 39.97, 40.25, 40.53, 40.81, 44.13, 46.40, 64.52, 97.73, 105.04, 108.58, 122.86, 124.01, 128.67, 130.21, 133.28, 148.85, 152.95, 154.32, 164.79, 167.94, 174.39; HRMS: calcd for $[M+H]^+$ $C_{35}H_{39}N_5O_4S_2$, 658.2522, found: 658.2568.

Cell culture and confocal fluorescence imaging

Cell culture

HeLa cells were cultured in Dulbecco's modified Eagle's medium (DMEM, Gibco) supplemented with 10% fetal bovine serum (HyClone) at 37 °C in a humidified incubator containing 5% CO_2 in air. The cells were passaged every two days at a ratio 1:5.

Fluorescence imaging of HeLa cells with the probE

2×10^4 mL^{-1} HeLa cells were seeded on uncoated glass bottomed dishes (Φ = 2 mm) for 24 h. After removing the medium, the cells were rinsed twice with PBS (pH = 7.2) and then treated with different concentrations of the probe (0.5, 2.5, 5 μM) for 2-6 h. Subsequently the cells were rinsed twice with PBS and fluorescence images were captured by confocal fluorescence microscope.

Co-location of the probe with lysosome in HeLa cells

HeLa cells were incubated with 5 μM probe RER for 6 h and then washed with PBS twice and loaded with lysosome tracker (1 μM) for 1 h. After removal of the lysosome tracker, the cells were rinsed PBS three times. Finally the images were obtained by confocal fluorescence microscope.

Imaging of pH changes within the lysosome

2×10^4 mL^{-1} HeLa cells were seeded on uncoated glass bottomed dishes (Φ = 2 mm) for 24 h and then pre-incubated with different concentrations of bafilomycin A1 for 6 h and treated with the probe (10 μM) for 4 h. Finally the cells were rinsed with PBS twice and captured by confocal fluorescence microscope.

Cytotoxicity assay

HeLa cells were seeded onto 96-well plates, then treated with 0.1% DMSO (as control) or **RE** or **RER** at 1, 5 and 10 μM for 24 h, respectively. Cell viability was performed by sulforhodamine B (SRB) protocol. Light absorption was measured at the wavelength of 540 nm using a SpectraMAX190 microplate spectrophotometer (GMI Co, USA).

Photo-bleaching Experiments

HeLa cells were seeded onto uncoated dish for 24 h, then treated with **RER** at 5 μM. Under continuously optimal light irradiation, the fluorescent images was captured by confocal fluorescence microscope after different time intervals (0, 15, 30, 60, 80, 100, 130, 200, 240, 300 s). The fluorescence intensity per cell was calculated by the formula: (Total fluorescence value - background fluorescence value)/cell number and quantified by the fluorescence analysis software ImageJ.

Conclusions

In summary, we have developed a rhodamine-rhodanine-based pH probe **RER** with pKa = 4.85 that is highly sensitive within the pH range of 4.1-7.2 and responds linearly to minor pH fluctuations from 4.2 to 5.2. The probe gives positive results when it was tested both in aqueous solution and in living cells. We proposed that the spiro structure of rhodamine opened upon protonation in weakly acidic conditions accompanied with fluorescence emission at 583.5 nm dramatically. Therefore, probe **RER** gives an obvious change in the fluorescence

intensity over a pH range and could be used to measure pH fluctuations in pathogenic cells and biological systems.

Acknowledgements

This study was supported by 973 Program (2010CB933504) and National Natural Science Foundation of China (91313303).

Notes and references

[a] Institute of Organic Chemistry, School of Chemistry and Chemical Engineering, Shandong University, Jinan 250100, P.R. China. E-mail addresses: bxzhao@sdu.edu.cn (B.X. Zhao); fax: +86 531 88564464; Tel.: +86 531 88366425

[b] Institute of Developmental Biology, School of Life Science, Shandong University, Jinan 250100, P.R. China. E-mail addresses: miaojy@sdu.edu.cn (J.Y. Miao)

† Equal contribution

Electronic Supplementary Information (ESI) available: Supplementary figures and characterization of the compound. See DOI: 10.1039/b000000x/

[1] R. MartínezZaguilán, B. F. Chinnock, S. Wald-Hopkins, M. Bernas, D. Way, M. Weinand, M. H. Witte and R. J. Gillies, *Cell. Physiol. Biochem.*, 1996, **6**, 169-184.
[2] S. Humez, M. Monet, F. Coppenolle, P. Delcourt and N. Prevarskaya, *Am. J. Physiol. Cell Physiol.*, 2004, **287**, 1733-1746.
[3] M. Czepán, Z. J. Rakonczay, A. Varró, I. Steele, R. Dimaline, N. Lertkowit, J. Lonovics, A. Schnúr, G. Biczó, A. Geisz, G. Lázár, Z. Simonka, V. Venglovecz, T. Wittmann and P. Hegyi, *Pflugers Arch.*, 2012, **463**, 459-475.
[4] J. K. Laihia, J. P. Kallio, P. Taimen, H. Kujari, V. M. Kähäri and L. Leino, *J. Invest. Dermatol.*, 2010, **130**, 2431-2439.
[5] J. W. Wojtkowiak and R. J, Gillies, *Autophagy*, 2012, **8**, 1688-1689.
[6] M. Lakadamyali, M. J. Rust, H. P. Babcock and X. Zhuang, *Proc. Natl. Acad. Sci. U. S. A.*, 2003, **100**, 9280-9285.
[7] K. R. Hoyt, I. J. Reynolds and *J. Neurochem.*, 1998, **71**, 1051–1058.
[8] R. A. Gottlieb, H. A. Giesing, J. Y. Zhu, R. L. Engler and B. M. Babior, Proc, *Natl. Acad. Sci. U. S. A.*, 1995, **92**, 5965-5968.
[9] A. Serafino, N. Moroni, R. Psaila, M. Zonfrillo, F. Andreola, F. Wannenes, L. Mercuri, G. Rasi and P. Pierimarchi, *Biochim. Biophys. Acta.,* 2012*,* **1822***,* 1004-1018.
[10] A. Rivinoja, N. Kokkonen, I. Kellokumpu and S. Kellokumpu, *J. Cell. Physiol.*, 2006, **208**, 167-174.
[11] J. Poschet, E. Perkett and V. Deretic, *Trends Mol. Med.*, 2002, **8**, 512-519.
[12] A. Kogot-Levin, M. Zeigler, A. Ornoy and G. Bach, *Pediatr. Res.*, 2009, **65**, 686-690.
[13] J. Han and K. Burgess, *Chem. Rev.*, 2010, **110**, 2709-2728.
[14] H. N. Kim, K. M. K. Swamy and J. Yoon, *Tetrahedron Lett.*, 2011, **52**, 2340-2343.
[15] V. Vingtdeux, M. Hamdane, S. Begard, A. Loyens, A. Delacourte, J. C. Beauvillain, L. Buee, P. Marambaud and N. Sergeant, *Neurobiol Dis.*, 2007, **25**, 686.
[16] H. S. Lv, S. Y. Huang, Y. Xu, X. Dai, J. Y. Miao and B. X. Zhao, *Bioorg. Med. Chem. Lett.*, 2014, **24** 535-538.
[17] R. Sun, W. Liu, Y. J. Xu, J. M. Lu, J. F. Ge and M. Ihara, *Chem. Commun.*, 2013, **49**, 10709-10711.
[18] W. S. Zou, Q. J. Shen, Y. Wang and W. J. Jin, *Chem. Res. Chin. Univ.*, 2008, **24**, 712-716.
[19] W. Liu, R. Sun, J. F. Ge, Y. J. Xu, Y. Xu, J. M. Lu, I. Itoh and M. Ihara, *Anal. Chem.*, 2013, **85**, 7419-7425.
[20] Z. Q. Hu, M. Li, M. D. Liu, W. M. Zhuang and G. K. Li, *Dyes Pigments*, 2013, **96**, 71-75.
[21] L. L. Long, X. F. Li, D. D. Zhang, S. C. Meng, J. F. Zhang, X. L. Sun, C. Zhang, L. P. Zhou and L. Wang, *RSC Adv.*, 2013, **3**, 12204-12209.
[22] S. Ohkuma and B. Poole, *Proc. Natl. Acad. Sci.*, 1978, **75**, 3327-3331.
[23] Q. J. Ma, H. P. Li, F. Yang, J. Zhang, X. F. Wu, Y. Baia and X. F. Li, *Sens. Actuators, B.*, 2012, **166-167**, 68-74.
[24] Y. Q. Tan, J. C. Yu, J. K. Gao, Y. J. Cui, Z. Y. Wang, Y. Yang and G. D. Qian, *RSC Adv.*, 2013, **3**, 4872-4875.
[25] L. J. Ma, W. G. Cao, J. L. Liu, D. Y. Deng, Y. Q. Wu, Y. H. Yan and L. T. Yang, *Sens. Actuators, B*, 2012, **169**, 243-247.
[26] K. M. Sun, C. K. McLaughlin, D. R. Lantero and R. A. Manderville, *J. Am. Chem. Soc.*, 2007, **129**, 1894-1895.
[27] D. W. Cui, X. H. Qian, F. Y. Liu and R. Zhang, *Org. Lett.*, 2004, **6**, 2757-2760.
[28] R. Pal and D. Parker, *Chem. Commun.*, 2007, 474-476.
[29] R. Huang, S. Y. Yan, X. L. Zheng, F. L. Luo, M. G. Deng, B. S. Fu, Y. J. Xiao, X. Zhao and X. Zhou, *Analyst*, 2012, **137**, 4418-4420.
[30] F. F. Han, Y. M. Xu, D. C. Jiang, Y. Qin and H. Y. Chen, *Anal. Biochem.*, 2013, **435**, 106-113.
[31] L. Q. Ying and B. P. Branchaud, *Bioorg. Med. Chem. Lett.*, 2011, **21**, 3546-3549.
[32] F. Yu, Y. Wang, W. C. Zhu, Y. Huang, M. H. Yang, H. Ai and Z. Y. Lu, *RSC Adv.*,2014, **4**, 36849-36853.
[33] L. Z. Chen, J. Li, Z. Z. Liu, Z. Ma, W. Zhang, L. P. Du, W. F. Xu, H. Fang and M. Y. Li, *RSC Adv.*, 2013, **3**, 13412-13416.
[34] K. K. Yu, K. Li, J. T. Hou, H. H. Qin, Y. M. Xie, C. H. Qian and X. Q. Yu, *RSC Adv.*,2014, **4**, 33975-33980.
[35] L. Yuan, W. Y. Lin, Z. M. Cao, J. L. Wang and B. Chen, *Chem. Eur. J.*, 2012, **18**, 1247-1255.
[36] H. S. Lv, J. Liu, J. Zhao, B. X. Zhao and J. Y. Miao, *Sens. Actuators, B.*, 2013, **177**, 956-963.
[37] Q. A. Best, R. Xu, M. E. McCarroll, L. Wang and D. J. Dyer, *Org. Lett.*, 2010, **12**, 3219-3221.
[38] X. L. Chen, X. M. Meng, S. X. Wang, Y. L. Cai, Y. F. Wu, Y. Feng, M. Z. Zhua and Q. X. Guo, *Dalton Trans.*, 2013, **42**, 14819-14825.
[39] J. L. Fan, C. Y. Lin, H. L. Li, P. Zhan, J. Y. Wang, S. Cui, M. M. Hu, G. H, Cheng and X. J. Peng, *Dyes Pigments,* 2013, **99**, 620-626.
[40] X. D. Liu, Y. Xu, R. Sun, Y. J. Xu, J. M. Lu and J. F. Ge, *Analyst*, 2013, **138**, 6542-6550.
[41] M. H. Lee, J. H. Han, J. H. Lee, N. Park, R. Kumar, C. Kang and J. S. Kim, *Angew. Chem. Int. Ed.* 2013, **52**, 6206-6209.
[42] J. L. Hu, F. Wu, S. Feng, J. H. Xu, Z. H. Xu, Y. Q. Chen, T. Tang, X. C. Weng and X. Zhou, *Sens. Actuators, B.*, 2014, **196**, 194-202.
[43] R. P. Haugland, A Guide to Fluorescent Probes and Labeling Technologies, Invitrogen Corp., The United States, 2005, pp. 580-588.
[44] H. S. Lv, S. Y. Huang, B. X. Zhao and J. Y. Miao, *Anal. Chim. Acta.,* 2013, **788**, 177-182.
[45] K. Bera, A. K. Das, M. Nag and S. Basak, *Anal. Chem.*, 2014, **86**, 2740-2746.
[46] C. A. Parker and W. T. Rees, *Analyst*, 1960, **85**, 587-600.
[47] Z. W. Xue, M. L. Chen, J. M. Chen, J. H. Han and S. F. Han, *RSC Adv.*, 2014, **4**, 374-378.
[48] W. S. Zhang, B. Tang, X. Liu, Y. Y. Liu, K. H. Xu, J. P. Ma, L. L. Tong and G. W. Yang, *Analyst*, 2009, **134**, 367-371.
[49] N. B. Yapici, S. R. Mandalapu, T. L. Chew, S. Khuon and L. Bi, *Bioorg. Med. Chem. Lett.,* 2012, **22**, 2440-2443.
[50] S. B. Wang, Y. F. Zhao, W. F. Zhu, Y. Liu, K. X. Guo and P. Gong, *Arch. Pharm. Chem. Life Sci*., 2012, **345**, 73-80.
[51] B. S. Zimenkovskii, M. I. Ganitkevich and I. M. Fedechko, *Farm. Zh. (Kiev)*., 1992, **2**, 34-7.

